

14th International Conference on Narrow Gap Semiconductors and Systems

Long wavelength electrically pumped GaSb-based Buried Tunnel Junction VCSELs

Alexander Bachmann^{a*}, Shamsul Arafin^a, Kaveh Kashani-Shirazi^a and
Markus-Christian Amann^a

^aWalter Schottky Institut, Technische Universität München, Am Coulombwall 3, 85748 Garching, Germany

Abstract

Long wavelength lasers are attractive light sources for free-space communications, military countermeasures, medical applications and trace-gas sensing systems by tunable diode laser absorption spectroscopy (TDLAS). As technically important gases, such as CO, CO₂ or CH₄, show strong absorption lines in a wavelength range from 2 to 3.5 μm, one is interested in the development of lasers emitting in that region. The (AlGaIn)(AsSb) material-system based on GaSb is the material of choice for devices in the near- to mid-infrared spectral region. In this paper, we present the device structure, design and results of an electrically-pumped GaSb-based VCSEL. The devices consist of an epitaxial GaSb / AlAsSb distributed Bragg reflector (DBR), a GaInAsSb quantum well gain section, a dielectric top DBR and a buried tunnel junction (BTJ) for electrical as well as optical confinement. Continuous-wave (cw) single-mode emission has been achieved up to a record high ambient temperature of 90°C. The wavelength is (electro-) thermally tunable from 2345 nm to 2365 nm. A maximum output power of 800 μW has been measured at 0°C.

Keywords: VCSEL; GaSb; infrared; TDLAS

1. Introduction

GaSb-based diode lasers emitting in the 2.0 – 3.3 μm wavelength range have drawn lots of attention for applications such as free-space communications, military countermeasures, medicine and trace-gas sensing by TDLAS. The latter technology shows huge potential for security applications as well as environmental monitoring and measuring techniques, and offers tremendous benefits for the detection of gases compared to state-of-the-art electrochemical sensors, such as rapid response time, long term stability, high selectivity and sensitivity. The method uses the fact that numerous gases have strong absorption lines in the near- to mid-infrared spectral range. These molecule resonances cause characteristic "fingerprints" in the detected light vs. current (*L-I*)-characteristics of the laser, as the laser's wavelength tunes over several nanometres while changing the bias current and therefore light

* Corresponding author. Tel.: +49-(0)89-289-12788; fax: +49-(0)89-3206620.
E-mail address: bachmann@wsi.tum.de.

is absorbed if the resonance is hit. By analyzing these dips in the $L-I$ -characteristics, gas concentrations may be calculated precisely using Lambert-Beer's law. For this technology, vertical-cavity surface-emitting lasers (VCSELs) offer key advantages, for instance their inherent longitudinal single-mode emission, low power consumption, efficient (electro-) thermal tunability and on-wafer testing capability. GaAs- and InP-based VCSELs have already been proven application-suited in the 0.65-2.3 μm range [1,2], but for emission in the longer wavelength regime novel materials have to be used. One possibility to realise single-mode surface emitting devices with long emission wavelengths are GaSb-based VCSELs, for which impressive results have already been obtained with optically pumped structures [3,4] and electrically pumped devices [5,6]. In this work, a device concept for an electrically pumped VCSEL on GaSb substrate is introduced. It utilizes the buried tunnel-junction (BTJ) approach. Compared to our previously reported lasers [6], improved characteristics relating to maximum operating temperature and output power are presented.

2. Device design

The device structure of the GaSb-based BTJ-VCSEL is shown in Fig. 1. The growth of the laser is divided into two parts, both performed by molecular beam epitaxy (MBE) in a Varian Gen II system. In the first growth step, the epitaxial DBR consisting of 24 pairs of GaSb:Te and AlAsSb:Te quarterwave layers, the active region and the tunnel-junction are deposited. The active region is formed by 5 compressively strained, 11 nm thick $\text{Ga}_{0.63}\text{In}_{0.37}\text{As}_{0.11}\text{Sb}_{0.89}$ quantum wells separated by 8 nm $\text{Al}_{0.33}\text{Ga}_{0.67}\text{As}_{0.03}\text{Sb}_{0.97}$ barrier material. The tunnel-junction layers are made of p^+ -GaSb and n^+ -InAsSb. As silicon acts as a donor in InAsSb and as an acceptor in GaSb, it can be used as dopant on both sides of the tunnel-junction, forming a low-resistive intra-device contact structure [7].

After the first growth, the tunnel-junction is dry-chemically etched and overgrown with n -doped GaSb in the second MBE growth-step. The structured tunnel-junction provides current-confinement by a low resistive contact in the inner part of the device, whereas in the etched regions a reversely biased (low doped) pn -junction is formed, blocking the current flow in the perimeter. Besides that, a key feature of the buried tunnel-junction is the substitution of p -doped layers by n -doped ones with their lower ohmic losses and suppressed intravalence-band absorption. On top of the BTJ and below the active region, n -type GaSb current- and heat-spreading layers are located, reducing ohmic losses and improving heat-sinking. To form the cavity of the VCSEL, a dielectric DBR consisting of 3 pairs of SiO_2 and amorphous Si is deposited by e-beam evaporation. Mesas are etched and passivated by sputtered SiO_2 . Semiconductor-metal contacts are formed by an n^{++} -InAsSb layer and e-beam evaporated Ti/Pt/Au. Here, Ti serves as an adhesion layer and Pt as a diffusion barrier for Au.

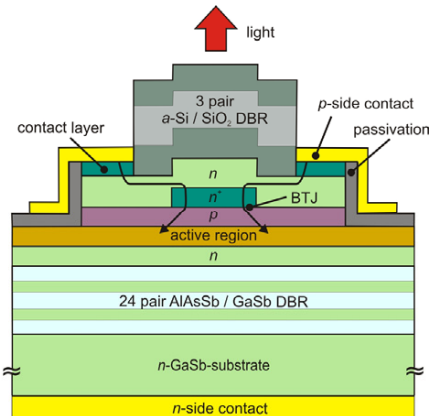


Fig. 1: Schematic structure of GaSb-based VCSEL. The cavity is formed by an epitaxial and a dielectric DBR. Key feature is a buried tunnel junction, providing current confinement as well as substitution of p -doped by n -doped layers for lower ohmic losses and reduced intravalence-band absorption. The schematic current flow is depicted with arrows.

3. Device results

The aim of the work described in this paper was the realization of VCSELs emitting around $2.35 \mu\text{m}$. At this wavelength, strong absorption lines of CO exist. As described in chapter 2, the structure was grown in two steps, while in between the tunnel junction layers were structured. Fig. 2a shows a reflectivity measurement after the second epitaxy step. For the measurement, the highly doped and therefore strongly absorbing contact layer has been removed from a part of the wafer. Clearly, reflectivity fringes from the epitaxial DBR and a stopband of about 69 meV width can be identified. Due to the cavity formed by the DBR and the $\approx 33\%$ reflection at the semiconductor – air interface, the resonance creates a dip within the stopband. However, the dip is not situated at the center of the stop band, which is due to layer thickness inaccuracy of the MBE and poor refractive index data given by the literature for this material-system. By simulation, the reflectivity spectra can reasonably be fitted to the measured one (see Fig. 2a). In order to achieve optimum reflectivity of the bottom mirror and to move the dip to the stopband center, the cavity was shortened. As shown by simulation in Fig. 2b, in this way the cavity resonance can be shifted from 519 meV to 526 meV by removal of 40 nm of the topmost GaSb-layer. This step was done by wet chemical etching. The laser emission of the realized device corresponds to the cavity resonance (see Fig. 2b).

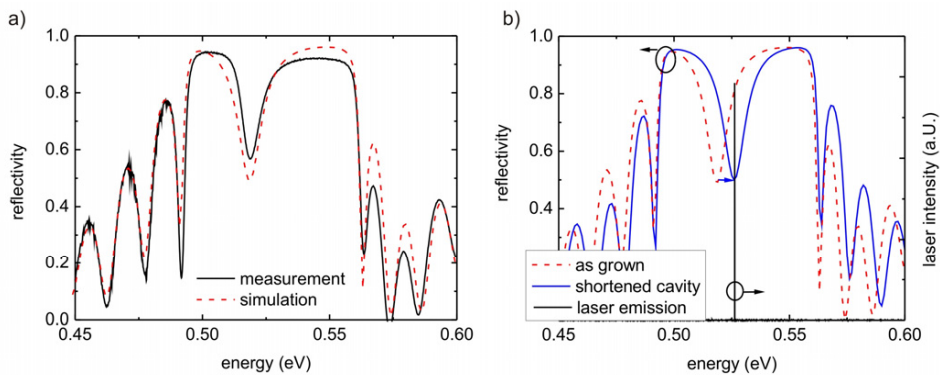


Fig. 2: (a) Measured and simulated reflectivity spectrum of a VCSEL wafer after the second epitaxy step and removal of the absorbing contact layer. As can be confirmed by simulation, the dip is located at too low energy due to a too thick cavity. (b) The reflectivity spectrum of the wafer, as grown (red, dotted) and after removal of 40 nm of the topmost GaSb-layer (blue). The dip shifts to larger energy. The laser emission of the device corresponds well to the cavity resonance.

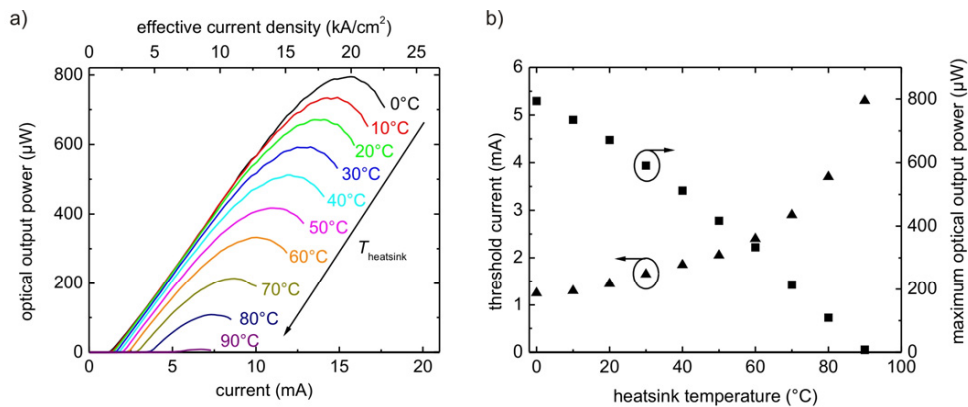


Fig. 3: (a) Temperature dependent L - I characteristics of a GaSb-based VCSEL with an elliptic BTJ of $6.44 \mu\text{m} \times 5.58 \mu\text{m}$ (axes diameters). (b) Threshold current and maximum optical output power vs. heatsink temperature.

L-I characteristics of the lasers were measured with a Peltier cooled InAs detector on a temperature controlled copper heatsink. In Fig. 3a, cw characteristics of a device with an elliptic aperture of $6.44 \mu\text{m} \times 5.58 \mu\text{m}$ (axes diameters) are shown. Laser emission up to 90°C has been recorded. At 0°C , the maximum output power is $800 \mu\text{W}$, and the threshold current is 1.2 mA , corresponding to an effective threshold current density of 1.5 kA/cm^2 , if a lateral diffusion of carriers of $2 \mu\text{m}$ on each side is taken into account. Fig. 3b depicts the characteristics of the threshold current and the maximum optical output power vs. the heatsink temperature. In VCSELs, the threshold current dependence on temperature is determined by the relative alignment of the gain maximum and the cavity resonance. Therefore, there is still potential for further device improvement concerning output power and maximum operating temperature by optimizing the mode-gain offset.

Spectra of the device were measured with a Vertex 70 (Bruker Optics GmbH) and a liquid nitrogen cooled InSb detector. Fig. 4a shows the spectra by varying the driving current at a constant heatsink temperature of 20°C . Single-mode operation has been achieved with a side-mode suppression ratio (SMSR) $> 25 \text{ dB}$. By electrothermal tuning, the emission wavelength tunes over a range of 10 nm (2348 nm to 2358 nm), yielding a tuning rate of 1.03 nm/mA (see Fig. 4b). Fig. 5a displays temperature dependent spectra at a constant driving current of 8 mA . A thermal tuning coefficient of 0.24 nm/K can be deduced (see Fig. 5b) and the device can be tuned over 20 nm in a temperature range from 0°C to 80°C . Due to the large accessible spectral range and the single-mode continuous-wave emission, the devices are very well suited for gas sensing applications. First measurements of CO have already been performed [8].

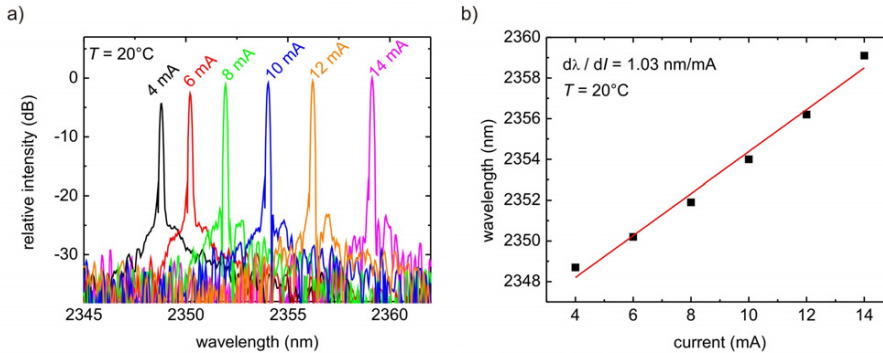


Fig. 4: (a) Spectra of VCSEL from Fig. 2 at different driving currents and constant heatsink temperature of 20°C , yielding single-mode operation with a SMSR $> 25\text{dB}$. (b) Wavelength tunability by changing the driving current, yielding a tuning rate of 1.03 nm/mA .

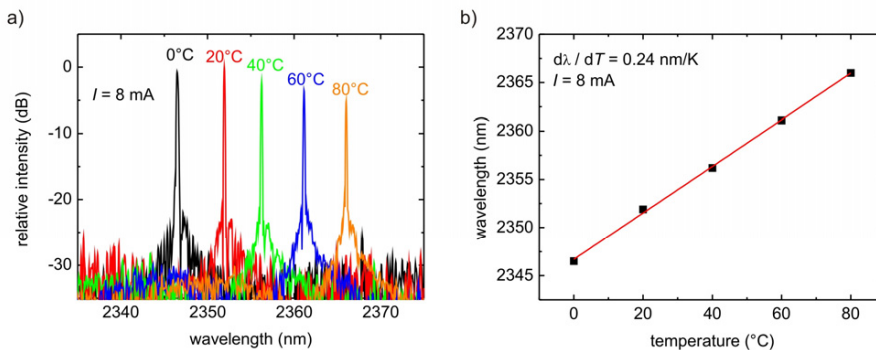


Fig. 5: (a) Spectra of VCSEL from Fig. 2 at varying heatsink temperature and constant driving current of 8 mA . (b) Wavelength tunability by changing the heatsink temperature, yielding a tuning rate of 0.24 nm/K .

Compared to our previously published devices [6], two major changes led to a better performance of the device: A reduction of the top mirror reflectivity from 99.8% to 99.5% by reducing the number of layer pairs from four to three increased the achievable output power. Secondly, the relative cavity resonance to peak gain offset has been improved by increasing the cavity thickness relating to the devices from [6]. Therefore, the emission wavelength has also been shifted by about 20 nm. The output power could be enlarged by a factor of 11. Despite the higher mirror losses, the effective threshold current density was kept constant because of the better matching of cavity mode and peak gain. Moreover, the maximum operating temperature is also shifted from 50°C to 90°C. Further improvement is expected by an additional increase of the mode-gain offset and a better matching of the active region and the tunnel junction position to the field anti-node and node, respectively. By that means, both threshold gain and optical losses in the highly absorbing BTJ layers can be reduced.

4. Conclusion

The device structure and results of an electrically pumped VCSEL based on GaSb were presented. For electrical and optical confinement, the device incorporates a buried tunnel junction. Continuous-wave operation around 2.36 μm has been achieved up to a record high stage temperature of 90°C. The longitudinally as well as transversely single mode emission is (electro-)thermally tunable over 20 nm making the device ideally suited for gas sensing applications by TDLAS. The presented device technology paves the way for the development of devices for the entire 2 – 3 μm wavelength range.

Acknowledgements

The authors gratefully acknowledge measurement support by VERTILAS GmbH. This work has been financially supported by the European Union via NEMIS (contract no. FP6-2005-IST-5-031845), the German Federal Ministry of Education and Research via NOSE (contract no. 13N8772) and the Excellence Cluster “Nanosystems Initiative Munich (NIM)”.

References

- [1] M. Ortsiefer et al., *Electron. Lett.* 42 (2006) 640-1.
- [2] B. Weigl et al., *IEEE J. Sel. Top. Quantum Electron.* 3 (1997) 409-15.
- [3] N. Schulz et al., *Phys. Stat. Sol. (c)* 3 (2006) 386-90.
- [4] L. Cerutti et al., *Electron. Lett.* 40 (2004) 869-70.
- [5] A. Ducanhez et al., *IEEE Phot. Technol. Lett.* 20 (2008) 1745-7.
- [6] A. Bachmann et al., *IEEE 21st Semiconductor Laser Conf.* (2008) 39-40.
- [7] O. Dier et al., *Electron. Lett.* 42 (2006) 419-20.
- [8] J. Chen et al., *Conf. in Lasers and Electro-Optics* (2009).